Title

SKA-31, an activator of Ca2+-activated K+ channels, improves cardiovascular function in aging.

Authors

John, Cini
Khaddaj Mallat, Rayan
Mishra, Ramesh
et al.

Publication Date

2020

DOI

10.1016/j.phrs.2019.104539

Peer reviewed

HHS Public Access

Author manuscript

Pharmacol Res. Author manuscript; available in PMC 2020 November 06.

Published in final edited form as:

Pharmacol Res. ; 151: 104539. doi:10.1016/j.phrs.2019.104539.

SKA-31, an activator of Ca^{2+}-activated K^+ channels, improves cardiovascular function in aging

Cini Mathew John[1,4,#], **Rayan Khaddaj Mallat**[1,4,#], **Ramesh C Mishra**[1,4], **Grace George**[1,4], **Vikrant Singh**[7], **Jeannine D Turnbull**[2,4], **Channakeshava S Umeshappa**[3], **Dylan J Kendrick**[1,4], **Taeyeob Kim**[1,4], **Fazlin M Fauzi**[6], **Frank Visser**[5], **Paul WM Fedak**[2,4], **Heike Wulff**[7], **Andrew P Braun**[1,4]

[1]Dept. of Physiology and Pharmacology, Cumming School of Medicine, University of Calgary

[2]Dept. of Cardiac Sciences, Cumming School of Medicine, University of Calgary

[3]Dept. of Microbiology, Immunology and Infectious Diseases, Cumming School of Medicine, University of Calgary

[4]Libin Cardiovascular Institute, Cumming School of Medicine, University of Calgary

[5]Hotchkiss Brain Institute, Cumming School of Medicine, University of Calgary

[6]Dept. of Pharmacology and Chemistry, Universiti Teknologi MARA, Malaysia

[7]Dept. of Pharmacology, University of California Davis, USA.

Abstract

Aging represents an independent risk factor for the development of cardiovascular disease, and is associated with complex structural and functional alterations in the vasculature, such as endothelial dysfunction. Small- and intermediate-conductance, Ca^{2+}-activated K^+ channels (KCa2.3 and KCa3.1, respectively) are prominently expressed in the vascular endothelium, and pharmacological activators of these channels induce robust vasodilation upon acute exposure in isolated arteries and intact animals. However, the effects of prolonged *in vivo* administration of such compounds are unknown. In our study, we hypothesized that such treatment would ameliorate aging-related cardiovascular deficits. Aged (~18 months) male Sprague Dawley rats were treated daily with either vehicle or the KCa channel activator SKA-31 (10 mg/kg, intraperitoneal injection; n=6/group) for 8 weeks, followed by echocardiography, arterial pressure myography, immune cell and plasma cytokine characterization, and tissue histology. Our results

*Author for correspondence: Dept. of Physiology and Pharmacology, Cumming School of Medicine, University of Calgary, 3330 Hospital Drive NW, Calgary, Alberta, CANADA T2N 4N1, Tel. # 403-220-8861, abraun@ucalgary.ca.

#These authors contributed equally to this study.

Author Contributions:

CMJ, RKM and APB conceived and designed the experiments. CMJ, RKM, RCM, JT, VS, FV, FMF, CSU, GG, TK, DK collected and/or analyzed the data. VS and HW synthesized SKA-31 and performed HPLC/MS. CMJ, RKM and RCM prepared a first draft of the manuscript, which was edited and revised by PWF, HW and APB.

Disclosures

The authors declare that they have no disclosures or competing financial interests related to this study.

show that SKA-31 administration improved endothelium-dependent vasodilation, reduced agonist-induced vascular contractility, and prevented the aging-associated declines in cardiac ejection fraction, stroke volume and fractional shortening, and further improved the expression of endothelial KCa channels and associated cell signalling components to levels similar to those observed in young male rats (~5 months at end of study). SKA-31 administration did not promote pro-inflammatory changes in either T cell populations or plasma cytokines/chemokines, and we observed no overt tissue histopathology in heart, kidney, aorta, brain, liver and spleen. SKA-31 treatment in young rats had little to no effect on vascular reactivity, select protein expression, tissue histology, plasma cytokines/chemokines or immune cell properties. Collectively, these data demonstrate that administration of the KCa channel activator SKA-31 improved aging-related cardiovascular function, without adversely affecting the immune system or promoting tissue toxicity.

Graphical Abstract

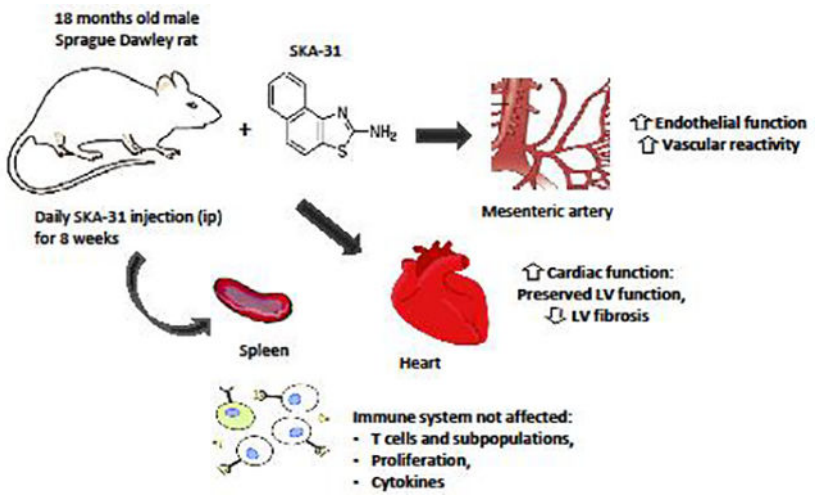

Keywords

Aging; Ca^{2+}-activated K^+ channels; Arteries; Heart; Immune system

1. Introduction

Aged individuals exhibit a higher incidence of morbidity and mortality as a result of cardiovascular disease (CVD), and normal aging itself represents a major independent risk factor for the development/progression of CVD, such as hypertension, atherosclerosis, stroke and coronary artery disease (1, 2). Physiologically, normal aging is associated with vascular endothelial cell dysfunction, which is often observed early in the progression of CVD (3–6). A hallmark feature of endothelial dysfunction is impaired endothelium-dependent vasodilation, which is commonly associated with reduced bioavailability of nitric oxide (NO), a key vasodilatory factor synthesized by the vascular endothelium. Impairment of NO production and/or its actions in the vascular wall is associated with arterial hypertension and increased atherogenesis (7, 8).

Another major vasodilatory signal in the vascular wall is endothelium-derived hyperpolarization (EDH), in which the activation of endothelial small- and intermediate-conductance, KCa channels (KCa2.3 and KCa3.1 channels, respectively) by Ca^{2+}-mobilizing, vasodilatory stimuli (e.g. acetylcholine and bradykinin) produces membrane hyperpolarization. This electrical signal then transfers to the surrounding vascular smooth muscle via myo-endothelial gap junctions to decrease the activity of L-type, voltage-gated Ca^{2+} channels (9–11), and the subsequent decline in cytosolic free Ca^{2+} promotes smooth muscle relaxation and increased vessel diameter. The EDH response acts in parallel with NO to promote vasodilation and lower systemic blood pressure. Functionally, EDH signaling can be directly stimulated in vascular tissue using selective, small molecule activators of KCa2.x and KCa3.1 channels (10, 12–14) and remains largely intact under pathologic conditions that compromise NO bioavailability and actions, e.g. type 2 diabetes (T2D) (15, 16). Indeed, we have reported that pharmacological “priming” of endothelial KCa channel activity can acutely restore normal endothelium-dependent vasodilation in coronary and mesenteric arteries from T2D (16). Such observations suggest that positive modulation of endothelial KCa channels can mitigate endothelial dysfunction, and may further oppose the development/progression of CVD in conditions, such as aging. However, the effects of prolonged *in vivo* administration of a KCa channel activator have yet to be examined. To investigate the potential benefit or risks of such a strategy, we treated ~18 month old male rats for 8 weeks with the well-characterized KCa channel activator, SKA-31 (17, 18) (10 mg/kg, daily I.P. injection), and examined its impact on cardiovascular performance *in vivo* and *in situ*, along with its effects on the immune system. Compared with vehicle-treated, aged controls, SKA-31 treatment reversed endothelial dysfunction in isolated, small mesenteric arteries, improved cardiac function, did not activate the immune system, or lead to overt tissue pathology. Western blotting and q-PCR analyses revealed that SKA-31 treatment positively regulated key signaling components in the vascular wall and T cells that collectively supported vasodilatory mechanisms and opposed pro-inflammatory signaling. Overall, measured parameters resembled those observed in young male rats. In summary, prolonged administration of SKA-31 was well tolerated in aged male rats, and improved cardiovascular performance without adversely affecting the immune system. This novel, proof-of-concept study thus provides a foundation to evaluate the potential therapeutic impact that KCa channel activators may have in reducing the development and/or progression of CVD.

2. Methods and Materials

2.1 Experimental animals & treatment

All procedures for animal treatment and care were conducted in accordance with the Guide for the Care and Use of Laboratory Animals of the National Institutes of Health (19), and were reviewed and approved by the University of Calgary Animal Care Committee. Young (~3 months of age at start of study) and aged male Sprague Dawley rats (~18 months of age at start) were treated with either drug vehicle or 10 mg/kg SKA-31 daily by intraperitoneal (I.P.) injection for 8 weeks. SKA-31 was synthesized as previously described (17) and dissolved in peanut oil (Sigma Aldrich) as a vehicle. In brief, peanut oil was heated in a sterile beaker on a magnetic stir plate to a temperature of ~60°C, followed by addition of

SKA-31 and constant stirring. Once the added SKA-31 had dissolved completely, heating was stopped and stirring was maintained. The final SKA-31 solution was allowed to cool to room temperature and appeared yellowish grey. The SKA-31 solution was then aliquoted into autoclaved 5 ml glass vials containing a mini-stir bar and stored at −20°C. Prior to injection, frozen SKA-31 solution was thawed, heated to ~60°C with stirring and then allowed to cool to room temperature. Rats were obtained from Charles River Laboratories (Montréal, PQ) and housed under standard conditions with regulated temperature and humidity and on a 12h/12h light/dark cycle. During the experimental process, rats were fed with certified standard rat chow and tap water ad libitum. Animals were monitored daily by veterinarians or trained technicians throughout the study for clinical signs of disease, such as weight loss, intractable diarrhea and opportunistic infection. Rats were euthanized by i.p. injection of sodium pentobarbital (50 mg/kg). Tissues and organs were collected according to the experimental protocols.

2.2 Isolation of mesenteric arteries and pressure myography

The mesentery vascular bed was excised and placed on a cooling plate containing ice-cold Krebs' solution containing (in mM): 115 NaCl, 4.7 KCl, 1 $MgSO_4$, 1 NaH_2PO_4, 25 $NaHCO_3$, 2.5 $CaCl_2$, pH adjusted to 7.4 with 1M NaOH. Third to fourth order branches of the arterial tree (300–350 micron internal passive diameter) were dissected, cleaned of adherent connective tissue, and transferred to an arterial pressure myography chamber (Living Systems, Burlington, VT). Individual vessels (~2 mm in length) were mounted on two glass cannulae fitted in the myography chamber, with each vessel end secured on a cannula by a 10.0 suture thread. The vessel lumen was filled with Krebs' solution containing 1 mg/ml bovine serum albumin. The cannulated artery was placed on the stage of an inverted microscope, and superfused with Krebs' buffer (gassed with 95% air/5% CO_2) at a flow of 7 ml/min using a peristaltic pump. A glass heat exchanger was used to warm the bubbled Krebs' solution to a bath temperature of 36–37°C. After 5–10 min equilibration, the intraluminal pressure of cannulated vessels was increased and then maintained at 70 mmHg throughout the experiment (no intraluminal flow was used). Following 15–20 min at 70 mmHg intraluminal pressure, arteries typically developed only a modest level of myogenic tone (i.e. <15% of maximal passive diameter), and were then stimulated with 1 μM phenylephrine to increase the extent of contraction. Continuous video measurement of the intraluminal vessel diameter was performed by a diameter tracking system (IonOptix, Milton, MA). Pharmacological agents were added to the bath via a peristaltic pump, as described (20).

2.3 Echocardiography

Echocardiographic analysis of heart function was conducted using an Esaote MyLab30 echocardiography system equipped with an 18 MHz transducer probe (Vet Gold, Indianapolis, USA). Rats were continuously anesthetized with inhalational 1.5–2% isoflurane and warmed on a heated pad (37°C); body temperature was monitored continuously using a rectal thermometer. For hydration, saline was injected subcutaneously (5% of the body weight of the animal), and eye gel was applied to keep the eyes moist. The chest area was shaved and then cleaned with isopropyl alcohol to improve imaging. Three lead needle electrodes were connected for continuous ECG monitoring. Ultrasound

transmission gel was applied to the chest and echocardiography (M-mode and B-mode imaging) was performed. Both two and four chamber views were utilized for analysis; systolic and diastolic diameters of the left ventricular chamber, interventricular septum and posterior wall thickness, as well as left ventricular fractional shortening, ejection fraction and stroke volume (calculated by area-length formula) were measured for each rat in a blinded manner. All values were averaged by using three to five cardiac cycles per rat.

2.4 Splenocyte isolation

Spleens were harvested from the rats following sacrifice. Splenocytes were prepared using a standard procedure as previously described (21, 22). Briefly, harvested spleens were washed with ice-cold PBS and stored in cold RPMI cell medium + 10% FBS. The spleens were gently pressed through a sterile wire sieve (70 μm pore size) over a Petri dish with 2 ml of RPMI medium using the plunger of a 5cc syringe. Disaggregated cells were transferred to a fresh tube and centrifuged at ~2000 rpm for 10 min. The cell pellet was re-suspended in 5 ml of red blood cell lysing buffer (BD Bioscience) and then incubated for 5–7 min at 37°C to ensure complete lysis. The remaining cells were washed with DPBS and re-suspended in complete media. Single splenocytes were used for flow cytometry analysis, sorting and proliferation assays.

2.5 Fluorescence-activated cell sorting

Splenocytes were labeled with anti-CD4 antibody (BV510; clone OX-35; BD Bioscience) following incubation for 20 minutes. CD4+T cells were gated according to FSC vs. SSC intensities. Gated CD4+ cells were further separated based on FSC-area vs. FSC height to discriminate singlet cells from doublets. Singlet cells with a purity <90% were sorted (23, 24) using a BD-FACS Aria II flow cytometer (BD Biosciences). The sorted cells were then used for western blot and qPCR analyses. Experimentally, T cells were gated as CD3+CD45RA- and further gated to double positive CD4+CD8+ T cells, CD4+CD8− helper T cells, CD4+CD25^{Hi}CD8− effectors, CD4-CD8+ cytotoxic T cells, CD4+CD25^{Hi}Foxp3+ regulatory T cells, and CD4-CD8+CD161^{Hi} NK T cells. B cells were gated as CD3-CD45RA+ in the lymphocyte population. The percentage of CD4+CD8− T cells is reported as a percentage of CD3+ T cells.

2.6 Tissue/cell preparation and western blot analyses

Mesenteric artery lysate was prepared using 4–5 arterial rings of similar size, as recently described (20). Freshly sorted CD4+ T cells (~5 × 10^6/ml) were placed in 1.5 ml Eppendorf tubes containing protein extraction buffer: 2M Tris HCl, pH= 6.8, 10 % glycerol, 2 % SDS, 0.01 % Bromophenol Blue. Following agitation, T cells were incubated at 95°C for 10 min, and then rotated at 4°C overnight in a cold room. The following day, cell lysates were aliquoted and snap-frozen at −80°C.

Homogenates prepared from isolated mesenteric resistance arteries and CD4+ T cells were separated by SDS polyacrylamide gel electrophoresis (PAGE) under constant voltage using a Hoefer mini-gel apparatus, and either 6%, 7.5% or 10% (w/v) acrylamide in the separating gel, as described (20, 25). Following electro-transfer, nitrocellulose membranes were incubated overnight at 4°C with affinity-purified primary antibodies (see Supplementary

Table 1 for antibody details). As we have observed that the anti-KCa3.1 monoclonal antibody used in our study can display non-specific, immunohistochemical staining in mouse brain (26), we validated the selectivity of this antibody in our Western blots by probing mesenteric arteries from wild-type and KCa3.1($^{-/-}$) global knockout mice (Supplementary Figure 1). Following incubation with primary antibodies, membranes were washed with TBS-T for 3 × 5 min at room temperature, and then incubated for 1–2 h at room temperature in TBS-T + 1% (w/v) milk powder containing peroxidase-conjugated goat anti-rabbit or anti-mouse IgG (Millipore catalogue# AP132P and AP124P, respectively). An enhanced chemiluminescence kit (Super Signal West Pico Plus, ThermoFisher Scientific) was used to detect antibody-labelled proteins. Immuno-labelled bands were quantified with a FujiFilm LAS3000 instrument and MultiGauge v3 software.

2.7 Detection of cell surface and intracellular markers by flow cytometry

Splenocytes (~1×10^6) were washed with staining buffer (0.05% (w/v) with sodium azide and 1% FBS in PBS) (BD Biosciences), followed by addition of 1 μl of CD32 as FC block, and then incubated for 30 minutes at 4°C. Cells were washed with staining buffer again, centrifuged at ~2000 × g for 10 min and re-suspended; 1 μl of surface antibodies conjugated with selected fluorochrome were added, followed by incubation for 30 minutes at 4°C (see Supplementary Table 2 for details of antibodies used for FACS protocol). Antibody labelled cells were then permeabilized using Fix-Perm buffer and washed with TF Perm buffer (BD Biosciences), followed by a 30 min incubation at 4°C with an intracellular stain for FoxP3 APC, and a final wash with DPBS. Single cells were suspended in 250 μl of PBS, and analyzed by FACScan, FACSaria, BD LSRII or Fortessa flow cytometers in combination with CellQuest Pro v5.1.1 software (BD Biosciences). The relevant isotype antibody controls were used in parallel with all primary measurements to establish negative gating parameters (27). Data analysis was performed using FlowJo v6.4.2 software (Tree Star, Inc.).

2.8 T cell proliferation assay

The *in vitro* cell proliferation assay was performed essentially as described (28). Splenocytes (~1×10^6) were stained with 0.25 μM CFSE (BD Bioscience) according to the manufacturer's directions and were either untreated or stimulated with 5 ng/ml PHA (Invitrogen/Gibco). Cells were maintained in 12 well plates for ~5 days following activation, and stained with anti-CD4 antibody. Proliferating CD4+ T cells were analyzed using a BD LSRII flow cytometer. The proliferative index for each cell population was determined using FlowJo v6.4.2 software.

2.9 Quantitative PCR

Total RNA was extracted from third to fourth order mesenteric arteries, and also from sorted CD4+ T cells, using a RNeasy micro kit (Qiagen), followed by generation of cDNA using a Quantinova cDNA synthesis kit (Qiagen). Quantitative PCR (q-PCR) was performed using primers from Integrated DNA Technologies (see Supplementary Table 3 for nucleotide sequences) and the Kapa SYBR Fast Universal qPCR kit (Kapa Biosystems). Rat glyceraldehyde 3-phosphate dehydrogenase (GAPDH) gene was used as the internal reference gene and counterchecked with β-actin (Actb). Control reactions and those

containing cDNA from mesenteric arteries were performed with 1 ng of template per reaction. The running protocol extended to 45 cycles consisting of 95°C for 5 s, 55°C for 10 s, and 72°C for 8 s using an Eppendorf Realplex 4 Mastercycler. PCR specificity was checked by dissociation curve analysis. Assay validation was confirmed by testing serial dilutions of pooled template cDNAs, indicating a linear dynamic range of 2.8–0.0028 ng of template and yielding percent efficiencies ranging from 100 – 118%. Control samples lacking template yielded no detectable fluorescence. Gene expression in tissue-derived RNA samples was determined using the relative expression software tool (REST) version 2.0.13 (29). Reporting of q-PCR data has been performed in accordance with the MIQE guidelines (30).

2.10 Quantification of cytokines and plasma constituents

Blood was collected by cardiac puncture on the day of sacrifice in 5 ml K_2EDTA-coated Vacutainer tubes (BD Biosciences), and cytokines were measured in isolated plasma. Multiplex arrays were performed with Luminex multi-analyte profiling (xMAP) technology. Plasma electrolytes, total protein, non-fasted glucose, testosterone and select diagnostic tissue enzymes were measured by IDEXX Laboratories (Markham, Ont.). Due to the collection of plasma in K_2EDTA-coated Vacutainer tubes, measurements of plasma K^+ and Ca^{2+} concentrations were deemed unreliable and are not reported.

2.11 Histopathology

Upon sacrifice, heart, aorta, spleen, kidney, liver and brain were collected and washed in ice cold PBS. Organs were kept in −20°C freezer for 1 hour to improve sectioning. The prepared organs were then stored in 4% paraformaldehyde (PFA) for 1 week. Subsequently, the organs were dehydrated and embedded in paraffin wax, and then cut into 5 micron thick sections using a microtome. Tissue staining with hematoxylineosin (H&E) (31) and Picro-sirius red (collagen stain) was performed as described (32). Stained tissues sections were visualized using an Olympus BX53 fluorescence-equipped microscope at 12.5x, 40x, 100x, 200x and 400x magnification, and images were digitally recorded. Collagen bundles were defined as bright yellow or orange coloured tissue under polarizing illumination. Typically, images taken under 200x or 400x magnification were used for analysis, with the aid of ImageJ software.

2.12 LC/MS analysis of SKA-31 concentrations

Commercial SPE cartridges (Hypersep C18, 100 mg, 1 mL, Thermo Scientific) were conditioned with acetonitrile, 2 × 1 mL, followed by 2 × 1 mL water. After loading the SPE cartridges with plasma samples, they were washed with 2 × 1 mL of 20% acetonitrile in water, followed by elution with a 2 × 1 mL of acetonitrile. Eluted fractions were collected and evaporated to dryness. The residues were suspended using acetonitrile and then subjected to LC-MS analysis.

Tissue samples were treated as follows: 4.0 mL of acetonitrile was added to 200 mg of tissue, which was then homogenized thoroughly using a T25 digital ULTRA-TURRAX homogenizer (IKA Works Inc.). The homogenized samples were centrifuged for 10 min at 4000 rpm, the supernatant was separated and evaporated under a constant air flow, followed

by reconstitution in acetonitrile. Reconstituted samples were loaded onto preconditioned SPE cartridges, and were then eluted with 2 mL of acetonitrile. Both load and eluted fractions were collected and evaporated to dryness. The residues were reconstituted to solution with 200 μL acetonitrile and used directly for LC-MS analysis.

LC/MS analysis was performed with a Waters Acquity UPLC equipped with a Acquity UPLC BEH C-18 column (1.7 μm, 2.1 × 50 mm) interfaced to a TSQ Quantum Access Max mass spectrometer (Thermo Fisher Scientific). The isocratic mobile phase consisted of 45% acetonitrile and 55% water, both containing 0.1% formic acid with a flow rate of 0.25 ml per minute. Using a heated electrospray ionization source (HESI II) in positive ion mode, capillary temperature 350°C, vaporizer temperature: 325°C, spray voltage 4000 V, sheath gas pressure (N2) 30 units, SKA-31 was analyzed by the selective reaction monitoring (SRM) transition of its molecular ion 201.04 $(M+1)^+$ into 115.16 m/z. A 9-point calibration curve with SKA-31 concentrations ranging from 25 nM to 5 μM was developed for quantification purposes (see Supplementary Figure 2). All analytic standards and samples were analysed in triplicate.

2.13 Data analysis and statistics

For pressure myography experiments, each artery was used for only a single experimental protocol. Data were evaluated using either one-way analysis of variance (ANOVA) or a Student's t-test, where appropriate. Multiple comparisons following ANOVA were performed using a Tukey's post-hoc test. All results are expressed as means ± S.D., with n indicating the number of experiments, with each experiment performed using tissue from a separate animal. Differences were considered statistically significant when $P < 0.05$.

3. Results

3.1 Functional enhancement of evoked vasodilation by SKA-31

We and others have observed that evoked vasodilation by endothelium-dependent agents, such as acetylcholine (ACh) or bradykinin (BK), can be significantly enhanced in the presence of a positive modulator/activator of KCa2.x and KCa3.1 channels (e.g. SKA-31, NS309) (16, 33), indicating that this class of compounds is able to augment the actions of a primary vasodilatory stimulus. In our study, young (~3 months at start) and aged (~18 months at start) male Sprague Dawley rats were treated daily for 8 weeks with either drug vehicle or a "threshold" dose of SKA-31 (i.e. 10 mg/kg) that was expected to have minimal effect on steady-state mean arterial blood pressure (17, 34). Based on cell and tissue studies, we predicted that this dose would "sensitize" endothelial KCa channel activation in response to endothelium-dependent vasodilatory stimuli (16, 33).

Arterial pressure myography was performed in pre-constricted, third and fourth order mesenteric arteries isolated from young and aged rats treated with either drug vehicle or 10 mg/kg SKA-31. As the focus of our study was the cardiovascular effect of SKA-31 in aging, vehicle treated young male rats (~5 months of age at end of study) served as a functional benchmark. The observed level of PE-induced pre-constriction (i.e. % change of maximal passive diameter) was significantly greater in vehicle-treated aged (44.3 ± 2.7%, mean ±

S.D., n=8) vs. young animals (38.1 ± 3.6%, n=12), whereas this vasoconstrictor response was reduced (36.5 ± 4.0%, n=8) in aged rats treated with SKA-31 (Fig 1A–D). SKA-31 treatment had no effect on PE-induced tone in mesenteric arteries from young rats (Supplementary Figure 3).

It is well established that aging induces endothelial dysfunction in the vasculature (4, 35). Acute stimulation of pre-constricted mesenteric arteries with vasodilatory agents acting primarily via the endothelium (i.e. ACh and BK), vascular smooth muscle (sodium nitroprusside, SNP and pinacidil, Pina) or both cell types (adenosine, ADO) was used to assess vascular responsiveness. As shown by the first half of the tracings in Fig. 1A and B, aged arteries (panel B) dilated less in response to ACh (0.3 μM) and BK (0.3 μM) compared with arteries from young rats. However, *in vivo* SKA-31 administration improved acute vasodilation evoked by ACh, BK and SNP in isolated arteries, yet, dilations evoked by either 10 μM ADO or 5 μM Pina were unaffected (Figure 1E). In contrast, SKA-31 treatment did not alter vasodilatory responses to ACh, BK or SNP in arteries from young animals (Supplementary Figure 3). Collectively, these results demonstrate that prolonged treatment with SKA-31 *in vivo* ameliorated endothelial dysfunction in mesenteric arteries from aged rats, and further reduced the magnitude of PE-induced vasoconstriction.

In isolated mesenteric arteries from vehicle-treated aged rats, acute exposure to a low concentration of SKA-31 (0.3 μM) significantly augmented vasodilation in response to ACh, BK and ADO (Fig. 1B and F, blue bars), whereas only the ACh response was enhanced in vessels obtained from vehicle-treated young rats (Fig. 1A and F, white bars). However, in arteries from aged rats treated with SKA-31, which exhibited significantly improved endothelium-dependent vasodilation, acute exposure to 0.3 μM SKA-31 did not augment vasodilatory responses to ACh, BK, ADO or SNP (Fig. 1C and F, red bars).

3.2 Upregulation of vascular proteins linked to KCa channel activity by SKA-31 treatment

Immunoblot analyses of key molecular components involved in agonist-evoked, endothelium-dependent vasodilation revealed that the expression of KCa2.3 and KCa3.1 channels, the sarco/endoplasmic reticulum Ca^{2+}-ATPase SERCA-2 and type 1 IP3 receptor (IP3R1) was reduced in aged mesenteric arteries, compared with young rats, whereas the expression of these same signalling components was significantly enhanced following *in vivo* SKA-31 administration (Fig. 2A–D). In contrast, the protein expression of endothelial NO synthase (eNOS), type 1α protein kinase G (PKG-1α), KCa1.1 (BKCa) channels and TRPV4 channels was similar in mesenteric arteries from vehicle-treated young and aged animals, and aged animals treated with SKA-31 (Fig 2E–H). SKA-31 treatment in young rats increased the expression of only KCa3.1 channel (Supplementary Figure 4). The mRNA levels of several of these same targets were also elevated in mesenteric arteries from SKA-31 treated young and aged rats, as revealed by qPCR analyses (Fig. 2I and Supplementary Figure 4). Functionally, pharmacological blockade of endothelial KCa2.3 and KCa3.1 channels impairs ACh-evoked relaxation in small mesenteric arteries from rat (20) (36). Together, these results demonstrate that SKA-31 administration enhanced the expression of endothelial KCa channels and associated proteins (e.g. SERCA-2 and IP3R1) that support agonist-evoked, Ca^{2+}-dependent vasodilation.

3.3 SKA-31 treatment improves cardiac structure and function in aged rats

Based on the observed improvement of vasoactive responses and protein expression in mesenteric arteries (Figs. 1 and 2), and the known systemic actions of SKA-31 following acute *in vivo* administration (14, 16, 17, 33, 34, 37, 38), we speculated that cardiac function and/or structure may also be improved in aged animals. Two-dimensional echocardiography (i.e. M-mode and B-mode) revealed that functional cardiac parameters (i.e. fractional shortening, LV ejection fraction and stroke volume) were significantly improved in aged rats treated with SKA-31, compared with vehicle treated controls (Fig. 3A–C, Supplementary Table 4 and Figure 6), and were equivalent to those values observed in vehicle-treated young rats. These observations are thus consistent with a well-documented, aging-related decline in cardiac performance (39, 40), and further suggest that prolonged SKA-31 administration may reverse/prevent such deficits in cardiac function. Importantly, SKA-31 administration did not alter heart rate in aged animals, suggesting no adverse effects on cardiac pacemaker function, electrical conduction or autonomic control (Fig. 3D). Histological analyses of the LV free wall from young and aged rats (Figs 3E–G) demonstrated that ventricular myocyte size significantly increased in aged animals (i.e. hypertrophy) (Fig. 3K), whereas myocyte density decreased (Figure 3L). Similarly, LV tissue from aged hearts displayed significantly elevated collagen content, as revealed by picrosirius staining (Fig 3O–R). Importantly, SKA-31 treatment abrogated these changes in aged animals. In young animals, SKA-31 treatment produced a modest increase in LV myocyte area without affecting myocyte density (Supplementary Figure 7).

Structural analyses of the thoracic aorta from young and aged rats revealed that the tunica medial (TM) layer (Fig. 3H–J), was significantly thicker in aged vs. young rats, and that this increase was reduced in aortae from SKA-31 treated rats (Fig. 3M). Thoracic aorta from aged animals also exhibited a lower density of vascular myocytes in the TM layer, which was not altered by SKA-31 treatment (Fig. 3N). These findings are consistent with the reported hypertrophy/remodeling of thoracic aorta with age (41–43), and indicate that SKA-31 treatment tended to normalize the vascular wall structure towards that of the young phenotype. In young rats, SKA-31 administration had no effect on either aortic thickness or myocyte density (Supplementary Figure 7). In cannulated mesenteric arteries from young and aged animals pressurized to 70 mmHg, arterial wall thickness measured under conditions of maximal passive dilation (i.e. nominally zero free external Ca^{2+}) was comparable and unaffected by SKA-31 treatment (Supplementary Figure 8).

3.4 Prolonged SKA-31 treatment does not promote a pro-inflammatory state

KCa3.1 channels are prominently expressed in both CD4+ and CD8+ T cells, where they regulate activation/proliferation, cell-mediated cytotoxicity, and volume (44, 45). As KCa3.1 channel inhibitors have been proposed as immunosuppressants and can inhibit T cell proliferation and cytokine production, it was important to examine whether long-term administration of SKA-31 may be pro-inflammatory in aged rats by promoting T cell activation. We therefore determined the frequency of different immune cell subsets in isolated splenocytes from vehicle and SKA-31 treated aged animals using flow cytometry. Remarkably, prolonged treatment of aged rats with SKA-31 did not change the observed frequencies of CD4+ T cells, CD8+ T cells, CD4+CD8+ double positive T cells, B cells, and

NK cells compared with age-matched, vehicle-treated rats (Fig. 4A–E). SKA-31 treatment also did not change the percentages of CD4+, CD8+ and regulatory T cells in young rats (Supplementary Figure 9). Collectively, these data indicate that long-term SKA-31 administration in aged rats does not change the population profiles of T cells.

Aging is also associated with low-grade, chronic inflammation (46–49) and broad spectrum analysis of T cell-associated cytokines/chemokines in the plasma from vehicle treated young and aged rats revealed an aging-related increase in pro-inflammatory markers, such as eotaxin, IL-6, IL-12, IL-13, IL-18, IP-10, MCP-1 and TNF-α (Fig. 4F and Supplementary Table 5). Importantly, prolonged SKA-31 treatment did not elevate these and other pro-inflammatory factors above the levels observed in vehicle treated aged rats, suggesting that low dose SKA-31 administration does not lead to broad elevation of proinflammatory cytokines, or overt activation of the immune system. SKA-31 administration also did not adversely affect plasma cytokine/chemokine levels in young animals (Supplementary Table 5).

3.5 SKA-31 treatment regulates the expression of Calcineurin-NFAT signaling factors

The calcineurin-NFAT pathway represents a major intracellular signaling cascade underlying T cell activation, proliferation and maintenance of immune responses (50). To investigate the integrity and activity of this pathway in vehicle and SKA-31 treated aged rats, CD4+ spleen cells were isolated, labeled with CFSE and cultured for ~5 days following stimulation with the mitogen phytohemagglutinin A (PHA). The proliferative index of PHA-stimulated T cells was measured via flow cytometry, and the results indicate that prolonged SKA-31 treatment did not significantly change the activation profile of splenic T-cells (Fig. 5A). In support of this functional result, western blot analyses indicated that NFAT-C1, calcineurin A subunit and SERCA2 protein levels were significantly reduced in CD4+ T cells from SKA-31 treated aged rats compared with vehicle treated controls (Fig. 5B–D), whereas the levels of other key signaling proteins (i.e. KCa3.1 channel, STIM1 and ORAI-1) were similar (Fig. 5E–G). Parallel qPCR analyses in these same T cell populations revealed significant decreases in the mRNA expression of several genes involved in Ca^{2+}-dependent T cell activation (e.g. calcineurin A subunit, NFAT-C1, phospholipase C-γ and Kv1.3 channel) (Fig. 5H). In young animals, SKA-31 treatment had no significant effect on the expression of these same targets either at the protein or mRNA levels (Supplementary Figure 10). H&E staining of fixed sections indicated that cell density was modestly decreased in intact spleens from aged rats, compared with vehicle-treated young rats, but was not further altered by prolonged SKA-31 treatment (Fig. 5I). Histological analyses of intact spleens also did not reveal any gross pathologic deficits (Fig. 5H–J) in vehicle- and SKA-31 treated aged animals (Fig. 5 J–L). Spleen histology and cell density were also unaffected by SKA-31 administration in young rats (Supplementary Figure 9).

3.6 Investigation of SKA-31 tissue distribution and potential toxicity.

In aged rats treated daily with SKA-31 (10 mg/kg) for 8 weeks, histopathological evaluation of fixed tissue sections did not reveal evidence of overt toxicity in heart, aorta, spleen, kidney, liver and cerebellum, compared with either vehicle-treated young and aged rats (Fig. 3E–J, Fig. 5J–L, Fig. 6A–I), which is further supported by quantitative assessment of

structural features, such as cell size, density and layer thickness (Fig. 6J–Q). Compared with vehicle-treated aged rats, SKA-31 treatment did not negatively affect glomerular size (i.e. area of glomerulus/Bowman's capsule) (Fig. 6J) or structure (i.e. area of Bowman's space/Bowman's capsule) (Fig. 6K) in the kidney, hepatocyte size and density in the liver (Fig. 6 L and M). In the cerebellum, long-term SKA-31 treatment did not adversely affect the thickness of either the molecular cell layer (Fig. 6N) or the granular cell layer (Fig. 6O), but did restore Purkinje cell area and density to the levels observed in young animals (Fig. 6P and Q). In young animals, SKA-31 treatment had no effect on tissue parameters in kidney, liver and brain (Supplementary Figure 7). At a whole body level, SKA-31 administration also did not alter the profile of plasma glucose, electrolytes, metabolites and testosterone (Supplementary Table 6), or change body weight, as both vehicle and SKA-31 treated aged rats exhibited similar weight gain over the course of our study (data not shown). The appearance of normal plasma levels of electrolytes, urea and total protein in SKA-31 treated animals further suggests an absence of drug-induced kidney dysfunction. In a previous study, acute exposure to SKA-31 (10 or 30 mg/kg i.p.) produced no overt signs of tissue toxicity in male Sprague Dawley rats (9–11 weeks of age) (17). Using HPLC/MS-based analyses, we further examined the plasma and tissue concentrations of SKA-31 at sacrifice following daily administration (10 mg/kg i.p.) for 8 weeks. Note that plasma and tissue samples were collected 16–18 h following the final SKA-31 injection. As illustrated in Fig. 6R, the highest concentration of SKA-31 was detected in abdominal adipose tissue (~1500 nM), whereas the SKA-31 concentrations observed in brain, liver and kidney ranged from 200–400 nM. In young animals, tissue concentrations of SKA-31 tended to be higher, although considerable variability was observed (Supplementary Figure 7). Plasma exhibited the lowest SKA-31 concentration (~50 nM) at time of sacrifice. Taken together, these data document the tissue distribution of SKA-31 following long-term administration, and further demonstrate that it does not substantially accumulate, or lead to off-target tissue damage.

4. Discussion

Acute exposure to SKA-31, a synthetic, positive modulator of KCa2.x and KCa3.1 channels (17) evokes acute vasodilation in isolated resistance arteries, increases flow in the coronary circulation, augments agonist-evoked dilation in endothelial dysfunction, and reduces systemic vascular resistance in intact animals (14, 16, 17, 33, 34, 37, 38). In the present study, we provide the first evidence that long-term, *in vivo* treatment (i.e. daily administration for 8 weeks) with SKA-31 positively influences cardiovascular function in healthy, aged male rats exhibiting moderate endothelial dysfunction. Strategies to reduce the negative consequences of endothelial dysfunction are predicted to oppose the development of CV disease (51, 52), and we rationalized that long-term administration of SKA-31 may mitigate/reverse the cardiovascular impairments associated with aging.

The results of our study demonstrate that: 1) Prolonged administration of SKA-31 reversed endothelial dysfunction in isolated mesenteric arteries from aged rats, reduced the magnitude of PE induced constriction, and enhanced the expression of endothelial KCa2.3 and KCa3.1 channels that support agonist-evoked, Ca^{2+}-dependent vasodilation, 2) The observed decline in cardiac function (i.e. reduced ejection fraction, stroke volume and fractional shortening) in aged rats was prevented with SKA-31 administration, 3) SKA-31

treatment did not lead to overt immune system activation, or promote proliferation in isolated splenic CD4+ T cells and 4) SKA-31 treatment did not lead to off-target tissue deficits or imbalances in plasma electrolytes or metabolites. SKA-31 administration in young animals had little or no effect on vascular responsiveness/protein expression, immune system activation or tissue histology.

In comparison with young (~5 months old) male rats, aged rats (~20 months old) exhibited vascular dysfunction, as shown by reduced vasodilatory responses to ACh and BK, and an elevated vasoconstrictor response to PE in small mesenteric arteries (Fig. 1), which were reversed following treatment of aged animals with SKA-31. Acute exposure of mesenteric arteries from aged rats to a low concentration of SKA-31 (0.3 μM) augmented endothelium-dependent vasodilation (Fig. 1). However, a similar effect was not observed in isolated arteries from either young or SKA-31 treated aged rats, suggesting that endothelial dysfunction was minimal in these latter groups. We and others have previously demonstrated that treatment of arteries from type 2 diabetic rodents with an activator of KCa channels (e.g. SKA-31, NS309) can counteract endothelial dysfunction, and improve agonist-evoked, endothelium-dependent vasodilation (15, 16). Endothelial dysfunction in vehicle-treated aged rats was associated with lower expression of key proteins involved in agonist-evoked, endothelium-dependent vasodilation (e.g. KCa2.3 and KCa3.1 channels, SERCA-2, type 1 IP3 receptor) (Fig. 2), whereas *in vivo* SKA-31 administration restored these protein levels in aged rats to those seen in young animals. The mRNA levels of these and other cellular components that participate in vasodilatory signalling were similarly elevated in mesenteric arteries from SKA-31 treated aged rats. Mechanistically, improvements in the vascular expression of key signalling factors are predicted to contribute to the reversal of endothelial dysfunction in aged animals following *in vivo* administration of SKA-31. It is further possible that some of these expression changes (e.g. SERCA-2) may occur in smooth muscle. It will be important to determine if other vascular beds (e.g. skeletal muscle, heart, brain) are similarly affected, as such effects may improve peripheral vascular responsiveness that would benefit cardiac function.

Assessment of *in vivo* cardiac performance by echocardiography (i.e. B-mode and M-mode imaging) revealed mild dysfunction in aged vs. young animals, as indicated by significant decreases in LV fractional shortening, ejection fraction and stroke volume (Fig. 3A–C). Aged male rats also exhibited modest LV hypertrophy, as revealed by histological examination (Fig. 3E–G, K, L). Importantly, these age-related changes were reversed following long-term SKA-31 administration, although our data do not reveal the mechanism(s) underlying this beneficial effect. Our finding that SKA-31 treatment reduced the age-related increase in left ventricular collagen content/fibrosis (Fig. 3R) likely contributes to the observed functional improvement in cardiac performance. It is further possible that beneficial effects of SKA-31 on peripheral vascular function with prolonged treatment could improve cardiac performance by lowering cardiac work and increasing O_2/nutrient delivery within the myocardium. Compared with young animals, we observed increased thoracic aortic wall thickness in aged rats, along with a modest decrease in vascular myocyte density (Fig. 3H–J and M-N); both findings are consistent with increased aortic/arterial stiffness in aging (53, 54). SKA-31 administration significantly reduced the increase in aortic wall thickness, without altering myocyte density. Elucidating the exact

mechanism(s) underlying these observed outcomes will require more focused investigation of the long-term hemodynamic effects associated with *in vivo* SKA-31 administration.

As KCa3.1 channels play a prominent role in T cell activation, proliferation and cytokine production via membrane hyperpolarization and augmented intracellular Ca^{2+} signaling (45), an important, yet unexplored question is whether prolonged SKA-31 administration adversely affects the immune system. Remarkably, we found that long-term SKA-31 treatment had no pro-inflammatory actions in either aged or young rats, based on the observed distribution and profiles of key T cell subpopulations (i.e. Treg, NK, T effector and T helper cells) and B cells (Fig. 4. A-E, Supplementary Fig. 9). Quantitative analyses of 30 major cytokines/chemokines revealed elevated plasma levels of several pro-inflammatory cytokines, such as eotaxin, interleukins 6,18 (IL-6, IL-18), Interferon gamma-induced protein 10 (IP-10), Monocyte chemo attractant protein-1 (MCP-1) and Tumor necrosis factor alpha (TNF-α) in aged rats, compared with young animals (Fig. 4F and Supplementary Table 5). These observations thus agree with reports of low-grade, chronic inflammation associated with aging (48, 55–57). SKA-31 treatment did not increase the plasma levels of pro-inflammatory factors in aged animals, blunted age-related increases in IL-18 and IP-10, and elevated the levels of the anti-inflammatory cytokine IL-4. SKA-31 administration also did not promote PHA-stimulated proliferation of isolated splenic CD4+ T cells (Fig. 5A), suggesting that these cells were not sensitized *in vivo* to proliferative stimuli. The observed decreases in the mRNA and protein expression of key molecules contributing to calcineurin-NFAT signaling in T cells from SKA-31 treated aged animals (Fig. 5B–H) may explain the absence of an enhanced stimulatory response with regards to T cell proliferation and cytokine production. SKA-31 treatment had no obvious effect on protein and mRNA expression in splenic CD4+ T cells from young animals (Supplementary Fig. 10). Collectively, these observations indicate that long-term SKA-31 administration in aged animals did not produce adverse effects on immune system activity.

Prolonged administration of SKA-31 was well-tolerated in both aged and young animals, as evidenced by the absence of gross tissue pathologies in the heart, aorta, kidneys, liver, spleen and cerebellum in aged animals (Figs. 3E–J, 5J–L, 6A–I, Supplementary Fig. 7), the presence of normal plasma electrolytes and glucose (Supplementary Table 6), normal weight gain over the study period, and no obvious changes in either behaviour or appearance. Reduced kidney and liver functions are also more common in aging, and such conditions could have led to higher plasma levels of SKA-31 in aged rats, due to decreased excretion and/or metabolism. However, plasma creatinine and liver enzyme levels in aged animals appeared normal (Supplementary Table 6), and the levels of SKA-31 in plasma and tissue at time of sacrifice did not suggest an accumulation of drug in aged animals. As SKA-31 is known to be brain-penetrant (17), it is interesting that SKA-31 treatment increased cerebellar Purkinje cell area and density in aged animals (Fig. 6P–Q). This finding is reminiscent of the neuroprotective effects of the related KCa channel activator riluzole (58), which is reported to affect multiple cation channels, including KCa2.x and KCa3.1 (17, 59, 60), and of the KCa2 channel selective activator NS13001, which has been shown to prevent neurodegeneration and improve motor performance in a mouse model of spinocerebellar ataxia (61).

Several experimental limitations in our study should be noted. Although the administration of 10 mg/kg SKA-31 has minimal effect on mean arterial blood pressure (≤ 5 mmHg) following acute i.p. injection in mice (17), it is unclear whether the same is true in aged rats following prolonged administration. If long-term SKA-31 treatment produced a modest decrease in systemic blood pressure (e.g. 5–10 mmHg) by improving vascular function/health, this primary effect could explain several of our observations. Another limitation of our study is our inability to establish cell specificity for the observed expression changes in target protein and mRNA in mesenteric arteries (i.e. endothelial vs smooth muscle) (Fig. 2) and isolated splenic T cells (Fig. 5). Such insights would increase our mechanistic understanding of the relation between the observed expression changes and cellular and tissue function.

Future studies are needed to examine how the SKA-31 mediated enhancement of vascular responsiveness in the mesentery, and possibly other vascular beds, contributes to the noted improvements in cardiac performance (i.e. ejection fraction, stroke volume, fractional shortening), and whether these effects are observable in females. The transcriptional/translational mechanism(s) by which prolonged SKA-31 administration leads to altered protein expression in the vascular wall and immune cells also deserves attention. One possibility is that SKA-31 administration initially improves cellular activity/function within select tissues (e.g. endothelial and smooth muscle cells) that over time feedbacks to positively regulate vascular mRNA and protein expression. These drug-mediated improvements in function could then positively influence cellular parameters such as oxidative stress, intracellular calcium levels, metabolism, or possibly systemic blood pressure, leading to beneficial regulation of vascular mRNA and protein expression, although we do not currently have data to support these possibilities. Enhancement of systemic blood pressure regulation by SKA-31 administration could also promote transcriptional/translational changes via mechanical stimulation of small arteries (e.g. changes in shear stress and/or wall tension). We thus speculate that the *in vivo* administration of SKA-31 indirectly affected the mRNA expression of multiple targets via its effects on cellular/tissue function, and did not act directly at either the genetic or transcriptional levels. Although no overt negative consequences of long-term SKA-31 administration were detected in our study, we remain cautiously optimistic, as we cannot completely rule out the possibility that SKA-31 treatment may have evoked an adverse event(s) that went undetected. In conclusion, this proof-of-concept study provides the first detailed evidence that long-term administration of a small molecule KCa channel activator (i.e. SKA-31) can improve cardiovascular function in aged male rats, without obvious safety and toxicity issues. These findings thus provide a platform to elucidate the cellular/tissue mechanisms underlying the putative beneficial effects of SKA-31 treatment on cardiovascular performance in aging.

Supplementary Material

Refer to Web version on PubMed Central for supplementary material.

Acknowledgements

The authors gratefully acknowledge Dr. Yong-Xiang Chen and the Libin Institute histopathology core facility for assistance with tissue staining, documentation and analyses, and Dr. Yiping Liu for technical assistance with flow cytometry. We also thank Dr. Michael Hill, University of Missouri, for his critical reading and feedback for the draft manuscript. The anti-SERCA2 and the anti-IP3R1 rabbit polyclonal antibodies were generously provided by Dr. Jonathan Lytton (University of Calgary) and Dr. David Yule (University of Rochester), respectively.

Funding: This study was supported by research funding to APB from the Canadian Institutes of Health Research (MOP-142467) and the Natural Sciences and Engineering Research Council of Canada (RGPIN-2017-04116), and to HW from the NIH (R21 NS101876). CMJ and RKM were supported in part by post-doctoral fellowship awards from the Libin Cardiovascular Institute and the Cumming School of Medicine, University of Calgary.

References

1. Lakatta EG, Levy D. Arterial and cardiac aging: major shareholders in cardiovascular disease enterprises: Part I: aging arteries: a “set up” for vascular disease. Circulation. 2003;107(1):139–146. [PubMed: 12515756]
2. Dai Z, Aoki T, Fukumoto Y, Shimokawa H. Coronary perivascular fibrosis is associated with impairment of coronary blood flow in patients with non-ischemic heart failure. J. Cardiol 2012;60(5):416–421. [PubMed: 22867802]
3. Donato AJ, Morgan RG, Walker AE, Lesniewski LA. Cellular and molecular biology of aging endothelial cells. Journal of Molecular and Cellular Cardiology. 2015;89(Pt B):122–135. [PubMed: 25655936]
4. Seals DR, Jablonski KL, Donato AJ. Aging and vascular endothelial function in humans. Clinical Science. 2011;120(9):357–375. [PubMed: 21244363]
5. Gates PE, Strain WD, Shore AC. Human endothelial function and microvascular ageing. Experimental Physiology 2009;94(3):311–316. [PubMed: 19042980]
6. Anderson TJ, Charbonneau F, Title LM, Buithieu J, Rose MS, Conradson H, Hildebrand K, Fung M, Verma S, Lonn EM. Microvascular function predicts cardiovascular events in primary prevention: long-term results from the Firefighters and Their Endothelium (FATE) study. Circulation. 2011;123(2):163–169. [PubMed: 21200002]
7. Vanhoutte PM, Zhao Y, Xu A, Leung SW. Thirty Years of Saying NO: Sources, Fate, Actions, and Misfortunes of the Endothelium-Derived Vasodilator Mediator. Circulation Research. 2016;119(2): 375–396. [PubMed: 27390338]
8. Vanhoutte PM, Shimokawa H, Félétou M, Tang EH. Endothelial dysfunction and vascular disease - a 30th anniversary update. Acta Physiologica. 2017;219(1):22–96. [PubMed: 26706498]
9. Félétou M, Huang Y, Vanhoutte PM. Endothelium-mediated control of vascular tone: COX-1 and COX-2 products. British Journal of Pharmacology. 2011;164(3):894–912. [PubMed: 21323907]
10. Köhler R, Olivan-Viguera A, Wulff H. Endothelial Small- and Intermediate-Conductance K Channels and Endothelium-Dependent Hyperpolarization as Drug Targets in Cardiovascular Disease. Adv. Pharmacol. 2016;77:65–104. [PubMed: 27451095]
11. Triggle CR, Samuel SM, Ravishankar S, Marei I, Arunachalam G, Ding H. The endothelium: influencing vascular smooth muscle in many ways. Canadian Journal of Physiology and Pharmacology. 2012;90(6):713–738. [PubMed: 22625870]
12. Brähler S, Kaistha A, Schmidt VJ, Wolfle SE, Busch C, Kaistha BP, Kacik M, Hasenau AL, Grgic I, Si H, Bond CT, Adelman JP, Wulff H, de Wit C, Hoyer J, Köhler R. Genetic deficit of SK3 and IK1 channels disrupts the endothelium-derived hyperpolarizing factor vasodilator pathway and causes hypertension. Circulation. 2009;119(17):2323–2332. [PubMed: 19380617]
13. Behringer EJ, Segal SS. Tuning electrical conduction along endothelial tubes of resistance arteries through Ca^{2+}-activated K^{+} channels. Circulation Research. 2012;110(10):1311–1321. [PubMed: 22492531]
14. Mishra RC, Mitchell JR, Gibbons-Kroeker C, Wulff H, Belenkie I, Tyberg JV, Braun AP. A pharmacologic activator of endothelial KCa channels increases systemic conductance and reduces arterial pressure in an anesthetized pig model. Vascular Pharmacology. 2016;79:24–31. [PubMed: 26239885]

15. Brondum E, Kold-Petersen H, Simonsen U, Aalkjaer C. NS309 restores EDHF-type relaxation in mesenteric small arteries from type 2 diabetic ZDF rats. British Journal of Pharmacology. 2010;159(1):154–165. [PubMed: 20015296]
16. Mishra RC, Wulff H, Cole WC, Braun AP. A pharmacologic activator of endothelial KCa channels enhances coronary flow in the hearts of type 2 diabetic rats. Journal of Molecular and Cellular Cardiology. 2014;72:364–373. [PubMed: 24787473]
17. Sankaranarayanan A, Raman G, Busch C, Schultz T, Zimin PI, Hoyer J, Köhler R, Wulff H. Naphtho[1,2-d]thiazol-2-ylamine (SKA-31), a new activator of KCa2 and KCa3.1 potassium channels, potentiates the endothelium-derived hyperpolarizing factor response and lowers blood pressure. Molecular Pharmacology. 2009;75(2):281–295. [PubMed: 18955585]
18. John CM, Mallat RK, George G, Kim T, Mishra RC, Braun AP. Pharmacologic targeting of endothelial Ca2+-activated K+ channels: A strategy to improve cardiovascular function. Channels. 2018;12(1):126–136. [PubMed: 29577810]
19. Grundy D Principles and standards for reporting animal experiments in The Journal of Physiology and Experimental Physiology. The Journal of Physiology. 2015;593(12):2547–2549. [PubMed: 26095019]
20. Khaddaj-Mallat R, Mathew John C, Braun AP. SKA-31, an activator of endothelial Ca^{2+}-activated K^+ channels evokes robust vasodilation in rat mesenteric arteries. European Journal of Pharmacology. 2018;831:60–67. [PubMed: 29753043]
21. Chiang EY, Li T, Jeet S, Peng I, Zhang J, Lee WP, DeVoss J, Caplazi P, Chen J, Warming S, Hackos DH, Mukund S, Koth CM, Grogan JL. Potassium channels Kv1.3 and KCa3.1 cooperatively and compensatorily regulate antigen-specific memory T cell functions. Nature Communications. 2017;8:14644.
22. John CM, Sandrasaigaran P, Tong CK, Adam A, Ramasamy R. Immunomodulatory activity of polyphenols derived from Cassia auriculata flowers in aged rats. Cellular Immunology. 2011;271(2):474–479. [PubMed: 21924708]
23. Harwani SC, Chapleau MW, Legge KL, Ballas ZK, Abboud FM. Neurohormonal modulation of the innate immune system is proinflammatory in the prehypertensive spontaneously hypertensive rat, a genetic model of essential hypertension. Circulation Research. 2012;111(9):1190–1197. [PubMed: 22904093]
24. Nanjundappa RH, Ronchi F, Wang JG, Clemente-Casares X, Yamanouchi J, Umeshappa CS, Yang Y, Blanco J, Bassolas-Molina H, Salas A, Khan H, Slattery RM, Wyss M, Mooser C, Macpherson AJ, Sycuro LK, Serra P, McKay DM, McCoy KD, Santamaria P. A Gut Microbial Mimic that Hijacks Diabetogenic Autoreactivity to Suppress Colitis. Cell. 2017;171(3):655–667. [PubMed: 29053971]
25. Swayze RD, Braun AP. A catalytically inactive mutant of type I cGMP-dependent protein kinase prevents enhancement of large conductance, calcium-sensitive K+ channels by sodium nitroprusside and cGMP. The Journal of Biological Chemistry. 2001;276(23):19729–19737. [PubMed: 11262387]
26. Jin LW, Lucente JD, Nguyen HM, Singh V, Singh L, Chavez M, Bushong T, Wulff H, Maezawa I. Repurposing the KCa3.1 inhibitor senicapoc for Alzheimer's disease. Ann. Clin. Transl. Neurol 2019;6(4):723–738. [PubMed: 31019997]
27. Kunnath-Velayudhan S, Porcelli SA. Isolation of intact RNA from murine CD4(+) T cells after intracellular cytokine staining and fluorescence-activated cell sorting. Journal of Immunological Methods. 2018;456:77–80. [PubMed: 29458078]
28. Wernimont SA, Wiemer AJ, Bennin DA, Monkley SJ, Ludwig T, Critchley DR, Huttenlocher A. Contact-Dependent T Cell Activation and T Cell Stopping Require Talin1. Journal of Immunology. 2011;187(12):6256–6267.
29. Pfaffl MW, Horgan GW, Dempfle L. Relative expression software tool (REST) for group-wise comparison and statistical analysis of relative expression results in real-time PCR. Nucleic Acids Research. 2002;30(9):e36. [PubMed: 11972351]
30. Bustin SA, Benes V, Garson JA, Hellemans J, Huggett J, Kubista M, Mueller R, Nolan T, Pfaffl MW, Shipley GL, Vandesompele J, Wittwer CT. The MIQE guidelines: minimum information for publication of quantitative real-time PCR experiments. Clinical Chemistry. 2009;55(4):611–622. [PubMed: 19246619]

31. Seibert TA, Hibbert B, Chen YX, Rayner K, Simard T, Hu T, Cuerrier CM, Zhao X, de Belleroche J, Chow BJ, Hawken S, Wilson KR, O'Brien ER. Serum heat shock protein 27 levels represent a potential therapeutic target for atherosclerosis: observations from a human cohort and treatment of female mice. Journal of the American College of Cardiology. 2013;62(16):1446–1454. [PubMed: 23764828]
32. Junqueira LC, Bignolas G, Brentani RR. Picrosirius staining plus polarization microscopy, a specific method for collagen detection in tissue sections. Histochem. J 1979;11(4):447–455. [PubMed: 91593]
33. Damkjaer M, Nielsen G, Bodendiek S, Staehr M, Gramsbergen JB, de Wit C, Jensen BL, Simonsen U, Bie P, Wulff H, Köhler R. Pharmacological activation of KCa3.1/KCa2.3 channels produces endothelial hyperpolarization and lowers blood pressure in conscious dogs. British Journal of Pharmacology. 2012;165(1):223–234. [PubMed: 21699504]
34. Radtke J, Schmidt K, Wulff H, Köhler R, de Wit C. Activation of KCa3.1 by SKA-31 induces arteriolar dilatation and lowers blood pressure in normo- and hypertensive connexin40-deficient mice. British Journal of Pharmacology. 2013;170(2):293–303. [PubMed: 23734697]
35. Behnke BJ, Delp MD. Aging blunts the dynamics of vasodilation in isolated skeletal muscle resistance vessels. Journal of Applied Physiology. 2010;108(1):14–20. [PubMed: 19797684]
36. Hilgers RH, Todd J Jr., Webb RC. Regional heterogeneity in acetylcholine-induced relaxation in rat vascular bed: role of calcium-activated K+ channels. American Journal of Physiology Heart and Circulatory Physiology. 2006;291(1):H216–222. [PubMed: 16473954]
37. Mishra RC, Belke D, Wulff H, Braun AP. SKA-31, a novel activator of SK(Ca) and IK(Ca) channels, increases coronary flow in male and female rat hearts. Cardiovascular Research. 2013;97(2):339–348. [PubMed: 23118129]
38. Mishra RC, Wulff H, Hill MA, Braun AP. Inhibition of myogenic tone in rat cremaster and cerebral arteries by SKA-31, an activator of endothelial KCa2.3 and KCa3.1 channels. Journal of Cardiovascular Pharmacology. 2015;66(1):118–127. [PubMed: 25815673]
39. Houghton D, Jones TW, Cassidy S, Siervo M, MacGowan GA, Trenell MI, Jakovljevic DG. The effect of age on the relationship between cardiac and vascular function. Mechanisms of Ageing and Development. 2016;153:1–6. [PubMed: 26590322]
40. Strait JB, Lakatta EG. Aging-associated cardiovascular changes and their relationship to heart failure. Heart Fail. Clin. 2012;8(1):143–164. [PubMed: 22108734]
41. Zhu BH, Guan YY, Min J, He H. Contractile responses of diabetic rat aorta to phenylephrine at different stages of diabetic duration. Acta Pharmacol. Sin. 2001;22(5):445–449. [PubMed: 11743894]
42. Hemmeryckx B, Hoylaerts MF, Deloose E, Van Hove CE, Fransen P, Bult H, Lijnen HR. Age-associated pro-inflammatory adaptations of the mouse thoracic aorta. Thrombosis and Haemostasis. 2013;110(4):785–794. [PubMed: 23925372]
43. Wheeler JB, Mukherjee R, Stroud RE, Jones JA, Ikonomidis JS. Relation of murine thoracic aortic structural and cellular changes with aging to passive and active mechanical properties. Journal of the American Heart Association. 2015;4(3):e001744. [PubMed: 25716945]
44. Ghanshani S, Wulff H, Miller MJ, Rohm H, Neben A, Gutman GA, Cahalan MD, Chandy KG. Up-regulation of the IKCa1 potassium channel during T-cell activation. Molecular mechanism and functional consequences. The Journal of Biological Chemistry. 2000;275(47):37137–37149. [PubMed: 10961988]
45. Feske S, Wulff H, Skolnik EY. Ion channels in innate and adaptive immunity. Annual Review of Immunology 2015;33:291–353.
46. Krabbe KS, Pedersen M, Bruunsgaard H. Inflammatory mediators in the elderly. Experimental Gerontology. 2004;39(5):687–699. [PubMed: 15130663]
47. Wang M, Jiang L, Monticone RE, Lakatta EG. Proinflammation: the key to arterial aging. Trends in Endocrinology and Metabolism. 2014;25(2):72–79. [PubMed: 24365513]
48. Goldberg EL, Dixit VD. Drivers of age-related inflammation and strategies for healthspan extension. Immunological Reviews. 2015;265(1):63–74. [PubMed: 25879284]
49. Ferrucci L, Fabbri E. Inflammageing: chronic inflammation in ageing, cardiovascular disease, and frailty. Nature Rev. Cardiol. 2018;15(9):505–522. [PubMed: 30065258]

50. Dienz O, Eaton SM, Krahl TJ, Diehl S, Charland C, Dodge J, Swain SL, Budd RC, Haynes L, Rincon M. Accumulation of NFAT mediates IL-2 expression in memory, but not naive, CD4+ T cells. Proc. Natl. Acad. Sci. U S A 2007;104(17):7175–7180. [PubMed: 17438271]
51. Veerasamy M, Bagnall A, Neely D, Allen J, Sinclair H, Kunadian V. Endothelial dysfunction and coronary artery disease: a state of the art review. Cardiology in Review. 2015;23(3):119–129. [PubMed: 25420051]
52. Seals DR Edward F. Adolph Distinguished Lecture: The remarkable anti-aging effects of aerobic exercise on systemic arteries. Journal of Applied Physiology. 2014;117(5):425–439. [PubMed: 24855137]
53. Seals DR, Kaplon RE, Gioscia-Ryan RA, LaRocca TJ. You're only as old as your arteries: translational strategies for preserving vascular endothelial function with aging. Physiology (Bethesda). 2014;29(4):250–264. [PubMed: 24985329]
54. Fleg JL, Strait J. Age-associated changes in cardiovascular structure and function: a fertile milieu for future disease. Heart Fail. Rev. 2012;17(4–5):545–554. [PubMed: 21809160]
55. Vasto S, Candore G, Balistreri CR, Caruso M, Colonna-Romano G, Grimaldi MP, Listi F, Nuzzo D, Lio D, Caruso C. Inflammatory networks in ageing, age-related diseases and longevity. Mechanisms of Ageing and Development. 2007;128(1):83–91. [PubMed: 17118425]
56. El Assar M, Angulo J, Rodriguez-Manas L. Oxidative stress and vascular inflammation in aging. Free Radical Biology & Medicine. 2013;65:380–401. [PubMed: 23851032]
57. Wang Z, Li J, Cho J, Malik AB. Prevention of vascular inflammation by nanoparticle targeting of adherent neutrophils. Nature Nanotechnology. 2014;9(3):204–210.
58. Cifra A, Mazzone GL, Nistri A. Riluzole: what it does to spinal and brainstem neurons and how it does it. Neuroscientist. 2013;19(2):137–144. [PubMed: 22596264]
59. Grunnet M, Jespersen T, Angelo K, Frokjaer-Jensen C, Klaerke DA, Olesen SP, Jensen BS. Pharmacological modulation of SK3 channels. Neuropharmacology. 2001;40(7):879–887. [PubMed: 11378158]
60. Cao YJ, Dreixler JC, Couey JJ, Houamed KM. Modulation of recombinant and native neuronal SK channels by the neuroprotective drug riluzole. European Journal of Pharmacology. 2002;449(1–2): 47–54. [PubMed: 12163105]
61. Kasumu AW, Hougaard C, Rode F, Jacobsen TA, Sabatier JM, Eriksen BL, Strobaek D, Liang X, Egorova P, Vorontsova D, Christophersen P, Ronn LC, Bezprozvanny I. Selective positive modulator of calcium-activated potassium channels exerts beneficial effects in a mouse model of spinocerebellar ataxia type 2. Chemical Biology 2012;19(10):1340–1353.

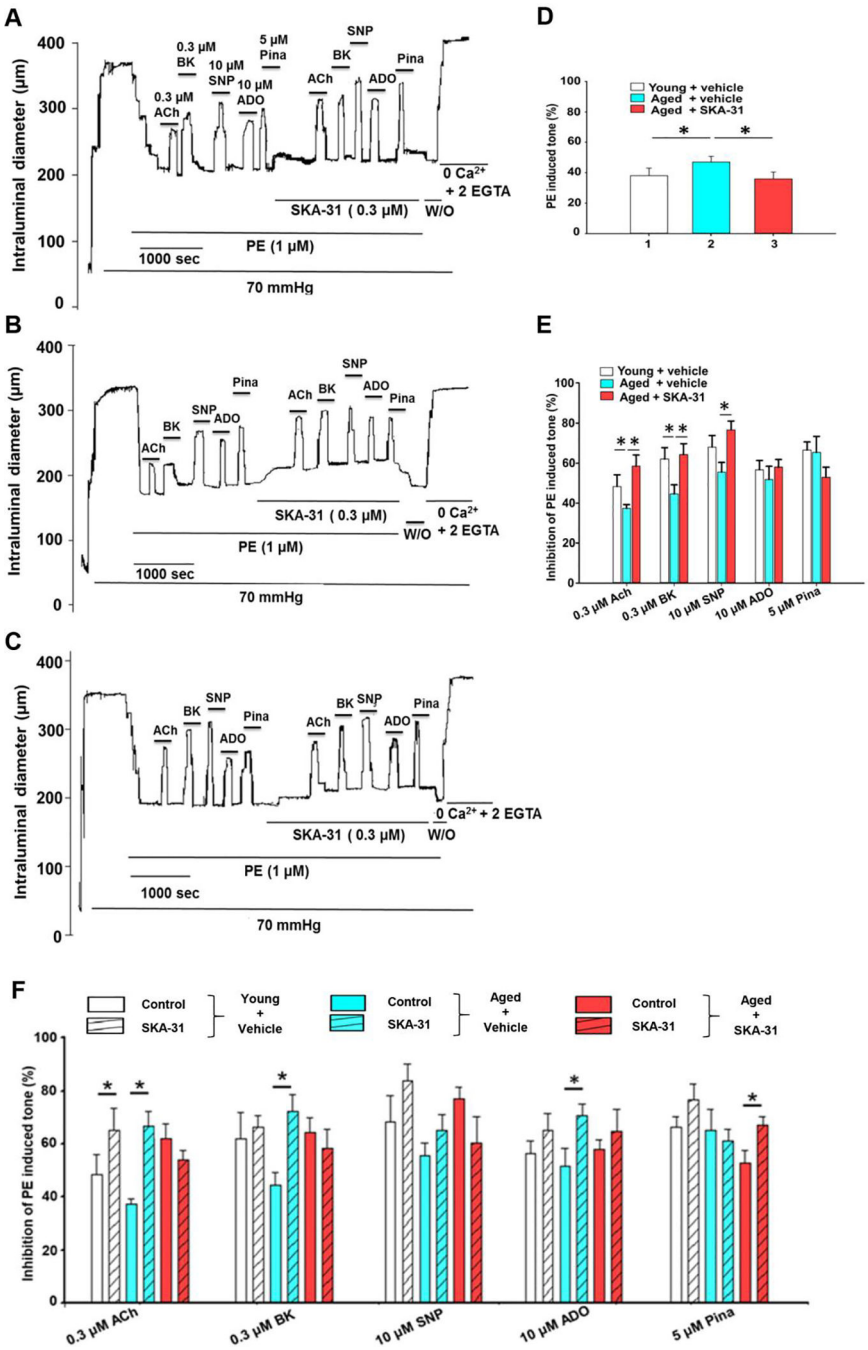

Figure 1 - SKA-31 administration improves vascular reactivity in isolated arteries.

Panels A-C display representative tracings showing vasodilatory responses evoked by acetylcholine (ACh, 0.3 μM), bradykinin (BK, 0.3 μM), sodium nitroprusside (SNP, 10 μM), adenosine (ADO, 10 μM) and pinacidil (Pina, 5 μM) in phenylephrine (PE) pre-constricted mesenteric arteries isolated from vehicle treated young (A), vehicle treated aged (B) and SKA-31 treated (10 mg/kg) aged male rats (C). The horizontal bars above and below the intraluminal diameter tracing indicate exposure to individual agents. In the second half of the protocol, arteries were acutely incubated with 0.3 μM SKA-31 to evaluate the potential

augmentation of evoked vasodilation. (D) Histogram quantifying the average PE-induced contractile tone (% of maximal intraluminal diameter) in mesenteric arteries isolated from vehicle and SKA treated aged rats, and vehicle treated young rats. Each bar represents the calculated mean ± S.D. (n = 4–5 animals). (E) Histogram quantifying the inhibition of PE induced tone in isolated mesenteric arteries (n = 4–5 arteries/condition, mean ± S.D). The asterisk (*) denotes a statistically significant difference between the indicated groups, as determined by ANOVA, $P < 0.05$. (F) Histogram quantifying the mean inhibitory response generated by vasodilatory agents in isolated mesenteric arteries from vehicle treated young rats, and either vehicle or SKA-31 treated aged rats, and in the absence (solid bar) and presence of 0.3 μM SKA-31 (striped bar) (means ± S.D., with n = 4–5 animals for each experimental condition). The asterisk (*) denotes a statistically significant difference vs. responses in the absence of SKA-31 exposure, as determined by a paired Student's t-test, $P < 0.05$.

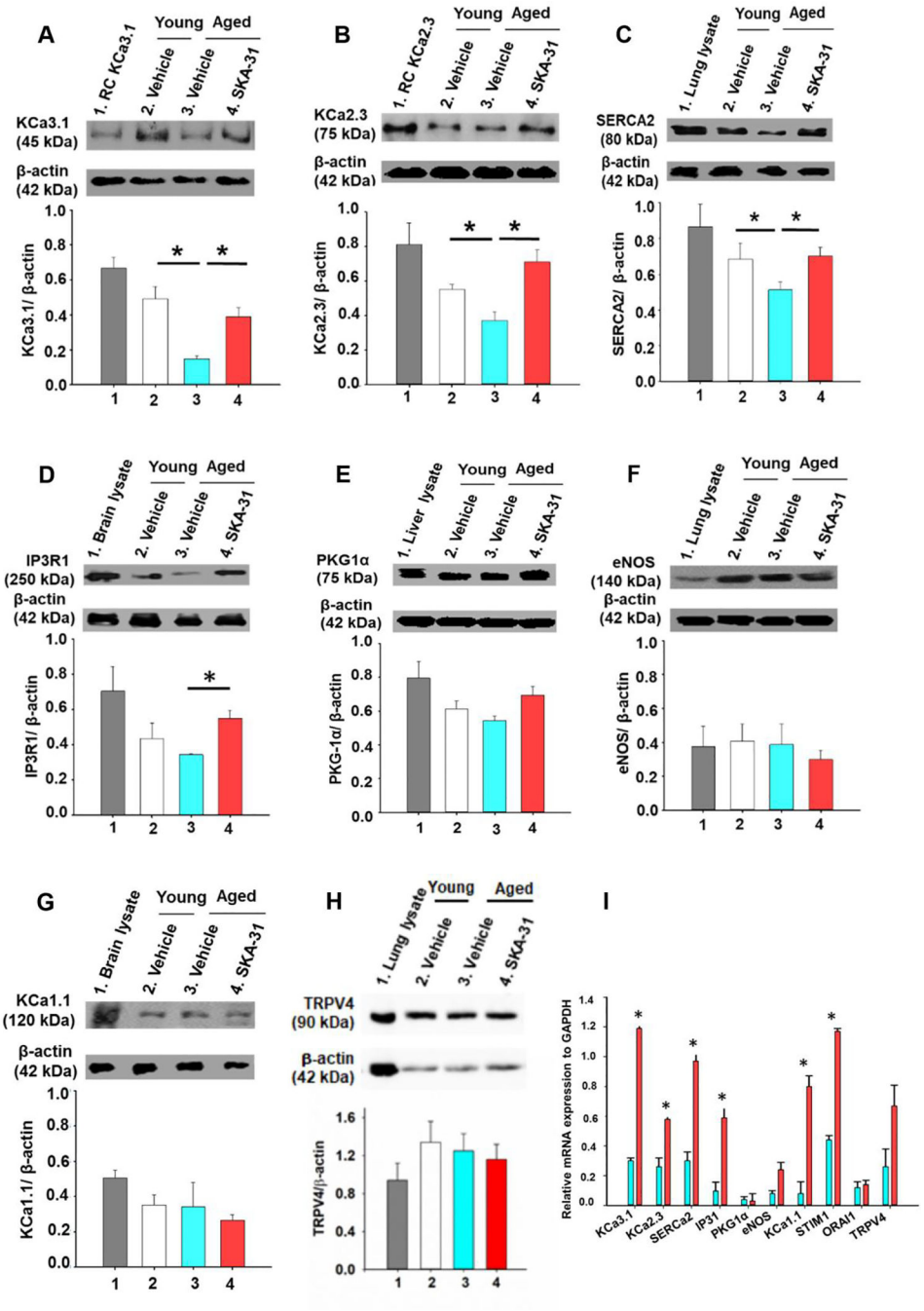

Figure 2 - SKA-31 administration modulates the expression of key proteins in mesenteric arteries.

Representative western blots and quantitative analysis of KCa3.1 channel (A), KCa2.3 channel (B), SERCA2 (C), type 1 IP3 receptor (IP3R1) (D), endothelial NO synthase (E), type 1α protein kinase G (PKG1α) (F), KCa1.1 channel (G) and TRPV4 channel (H) in mesenteric artery homogenates derived from vehicle treated young (white), vehicle treated aged (blue) and SKA-31 treated aged rats (red). For each primary antibody tested, a lysate derived from a tissue or recombinant cell (RC) line expressing the target protein was included as a positive control, and is displayed in lane 1 of each blot. Staining intensities of

the selected immuno-reactive bands are expressed as a ratio with detected β-actin expression in the same homogenate. The asterisk signifies a statistical difference between the indicated groups (n = 4–5 animals), as determined by ANOVA and a Tukey post-hoc test, $P < 0.05$. Full length, uncropped images of the blots displayed in this figure are presented in Supplementary Figure 5. Panel I shows the mRNA levels of key signaling proteins in mesenteric arteries from SKA-31 treated aged rats (red bars), in comparison with vehicle treated aged rats (blue bars), as determined by qPCR analysis. Data in aged animals are normalized to the expression level of the same target mRNA detected in mesenteric arteries from vehicle treated young rats; data normalization was calculated using REST software. GAPDH was utilized as an internal reference mRNA in all determinations. The asterisk indicates a statistically significant difference ($P < 0.05$) compared with vehicle treated aged rats, as determined by an unpaired Student's t-test (n = 4–5 animals/group).

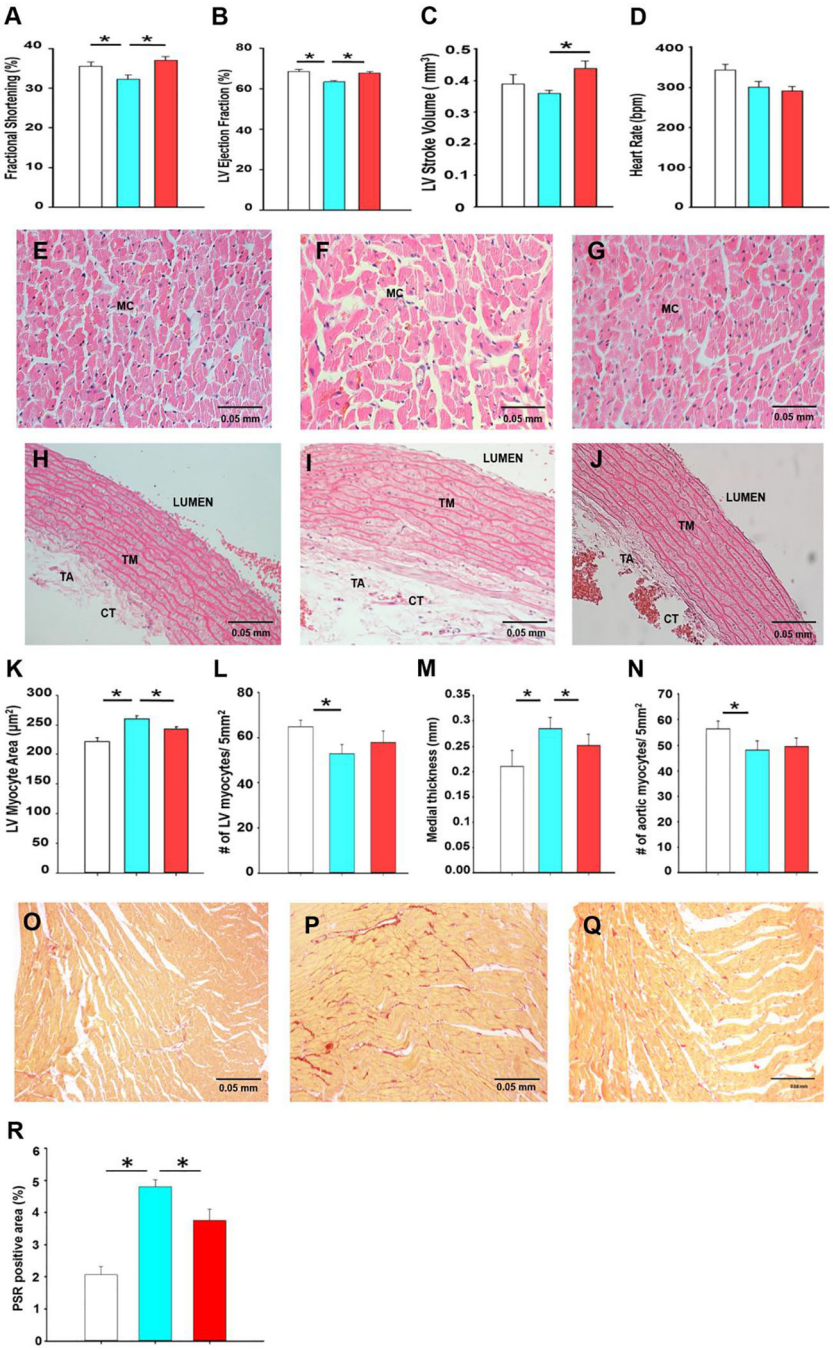

Figure 3 - SKA-31 treatment improves cardiovascular structure and function

Panels A-D depict primary parameters (i.e. fractional shortening, ejection fraction, stroke volume and heart rate) of cardiac function, as determined by echocardiographic imaging (B-mode and M-mode) and analyses, in vehicle treated young animals (white), vehicle (blue) and SKA-31 treated (red) aged rats. Data are expressed as means ± S.D. The asterisk indicates a statistically difference between the indicated groups, as determined by ANOVA and a Tukey's post-hoc test (n = 6 animals/group, $P^{<}$ 0.05). Panels E-G present H&E staining (400x magnification) of the left ventricular free wall from young rats (E), vehicle

(F) and SKA-31 treated aged rats (G). Scale bar in the bottom right corner of each image represents 50 microns; MC: myocyte. The H&E stained sections in panels H-J (400x magnification) depict cross sections of thoracic aorta isolated from young animals (H), vehicle (I) and SKA-31 treated aged rats (J). Scale bar in the bottom right corner of each image represents 50 microns; TA: tunica adventitia, TM: tunica media, CT: connective tissue. Panels K and L quantify the size of individual LV myocytes (n ≥50 cells analyzed per tissue) and the density/number of LV myocytes per $5mm^2$ of tissue area in the three treatment groups, respectively. Medial layer thickness of the thoracic aorta and the density/number of aortic myocytes per 5 mm^2 of tissue area are depicted in panels M and N, respectively. Colour coding as in panels A-D. Panels O-Q display representative picrosirius red-stained sections of the left ventricular (LV) free wall from young rats (O), vehicle (P) and SKA-31 treated aged rats (Q). Scale bar in the bottom right corner of each image represents 50 microns. The histogram in panel R quantifies the picrosirius red (PSR)-positive area in LV tissue from each group. Measurements of cell and tissue dimensions were performed using a manual tracing function in ImageJ. Statistical analysis was performed using one-way ANOVA, followed by a Tukey's post-hoc test (n = 6 animals); * denotes a statistically significant difference between the indicated groups, $P < 0.05$.

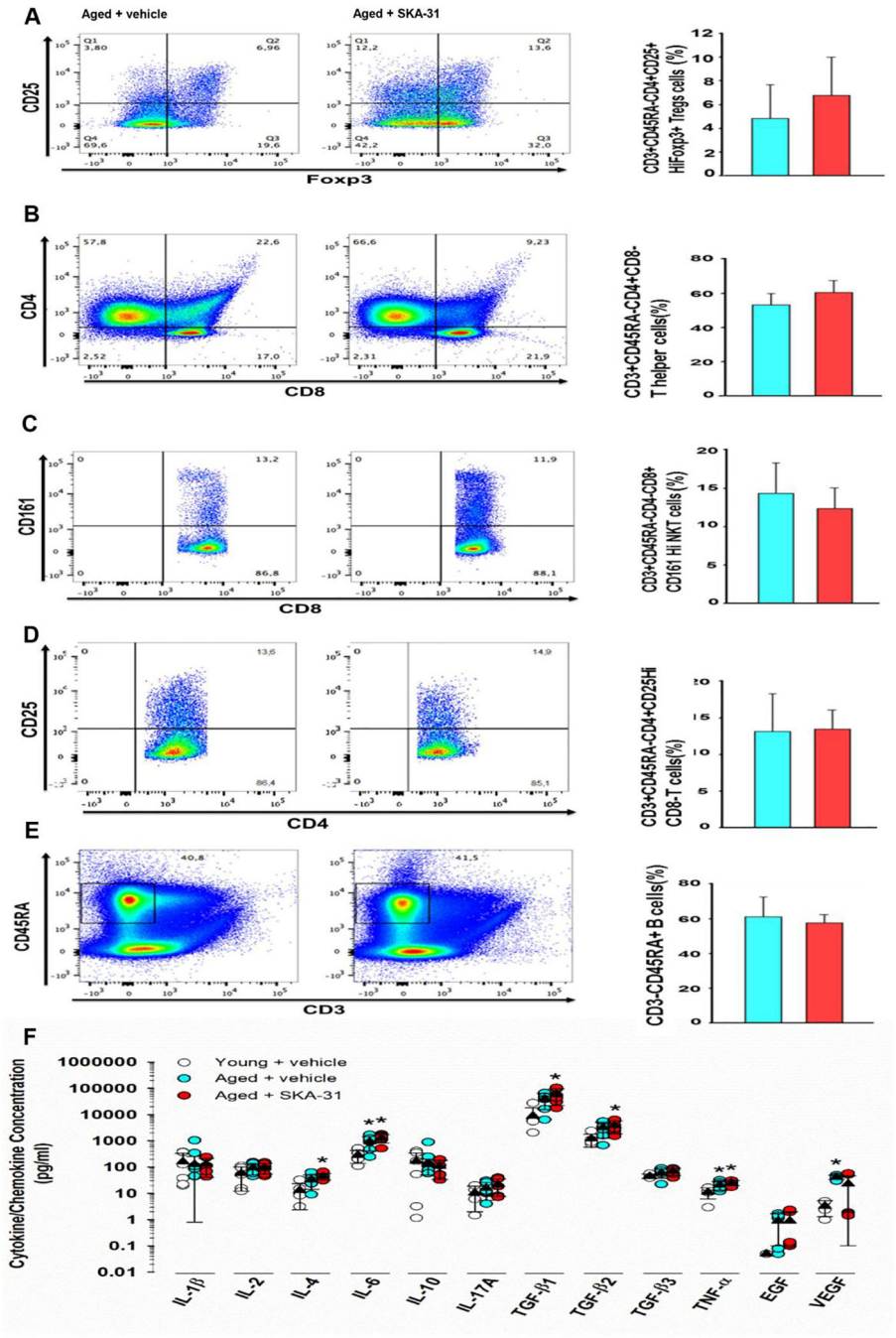

Figure 4 –. Long-term SKA-31 treatment does not promote a pro-inflammatory state

Panels A-E display representative flow cytometry profiles of immune cell subsets isolated from the spleens of vehicle (left column) and SKA-31 treated (middle column) aged rats, together with associated quantification (right column). In the lymphocyte population, T cells were gated as CD3+CD45RA- and further gated to regulatory T cells (CD4+CD25+HiFoxp3+, P = 0.063) (A), helper T cells (CD4+CD8−, P = 0.063) (B), NKT cells (CD4-CD8+CD161Hi, P = 0.463) (C), T effectors (CD4+CD25HiCD8−, P = 0.465) (D) and B cells (CD3-CD45RA+, P = 0.210) (E). Results displayed in histograms represent

the percentage of the parental population (i.e. the percentage of CD4+CD8− T cells is reported as a percentage of CD3+ T cells, not total T cells). Blue = vehicle treated aged rats, red = SKA-31 treated animals. The two groups were compared statistically using a Mann-Whitney test, and the data are expressed as means ± S.D. (n=6 animals). (F) Quantification of select cytokines/chemokines in plasma from vehicle and SKA-31 treated aged animals, and vehicle treated young rats. Vertically arranged data points represent individual concentration values in pg/ml for a given factor within a given treatment group, as identified in the legend, and are plotted on a logarithmic scale. Solid triangles and error bars indicate the mean ± S.D. for each factor/group. The presence of an asterisk above a symbol column denotes a statistically significant difference vs. the vehicle-treated young group, $P < 0.05$. The complete list of cytokines/chemokines measured in all three treatment groups is presented in Supplementary Table 5.

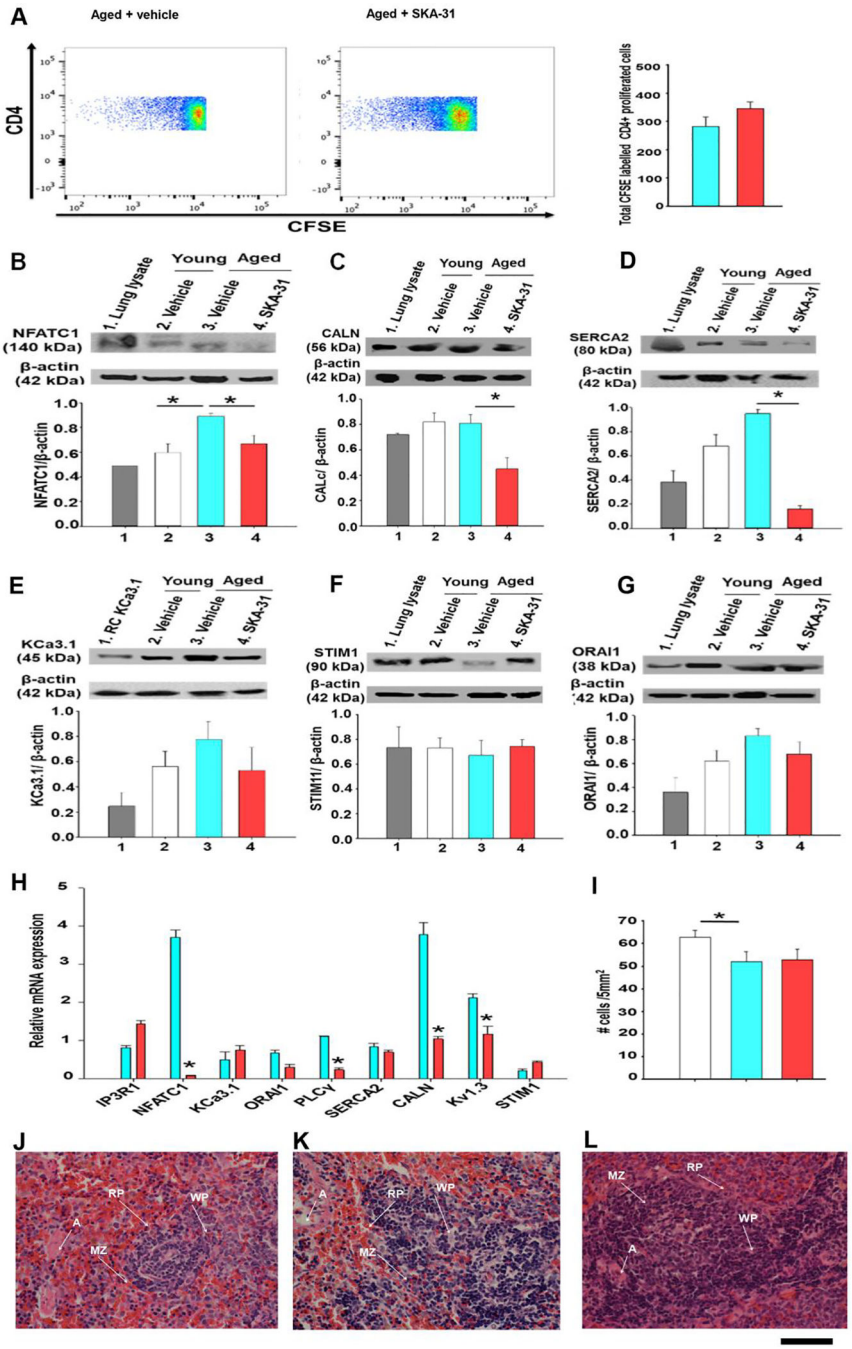

Figure 5 - SKA-31 administration regulates the expression of calcineurin/NFAT signaling components in T cells

Panel A displays representative FACS analysis of splenic lymphocytes (1×10^6 cells) isolated from vehicle and SKA-31 treated aged rats, which were first labeled with CFSE, stimulated with phytohemagglutinin A and cultured for ~5 days at 37°C. Cells were then labeled with anti-CD4 BV510 to enable discrimination between other splenic cells. Events (~200,000) were identified based on the fluorescence intensity above the background auto-fluorescence level, ensuring that only CFSE-positive events were analyzed. The selected fluorescence intensities reflect gating of the proliferative T cell population in each treatment group. Blue

represents the lowest fluorescence intensity; red represents the highest. The accompanying histogram depicts cell division in the T cell compartment, as revealed by anti-CD4+ staining. Blue = vehicle treated aged rats, red = SKA-31 treated animals. Panels B-G present western blot analysis and quantification of NFATC1 (B), calcineurin catalytic subunit (C), SERCA2 ATPase (D), KCa3.1 channel (E), STIM1 (F) and ORAI1 channel (G) in splenic CD4+ T cells from vehicle treated young (white), vehicle treated aged (blue) and SKA-31-treated aged rats (red). For each primary antibody tested, a lysate derived from a tissue or recombinant cell (RC) expressing the target protein was included as a positive control, and is displayed in lane 1 of each blot. Staining intensities of the various immuno-reactive bands detected in T cell homogenates are expressed as a function of β-actin (n = 4 animals/group). An asterisk signifies a statistically significant difference between the two indicated groups, as determined by one-way ANOVA and a Tukey's post-hoc test ($P < 0.05$). Note that full length, uncropped images of the blots displayed in this figure are presented in Supplementary Figure 11. Panel H displays the mRNA expression of key signaling proteins in splenic CD4+ T cells from vehicle (blue) and SKA-31 treated (red) aged rats. The qPCR results for each target have been normalized to the mRNA expression of the same gene observed in vehicle treated young animals; GAPDH was utilized as the internal reference gene for all qPCR analyses. Relative mRNA expression was calculated using REST software. An asterisk indicates a statistical difference compared with the vehicle treated aged rats, as determined by an unpaired Student's t-test ($P<0.05$) (n=3–5 animals/group). Panel I displays the quantification of cells per $5mm^2$ of H&E stained sections of intact spleen from vehicle treated young animals (white bars), vehicle (blue bars) and SKA-31 treated aged rats (red bars), as determined by ImageJ software (n=6 animals/group). Panels J-L show H&E staining of spleen sections (400x magnification) from vehicle treated young animals (J), vehicle (K) and SKA-31 treated (L) aged rats. The scale bar beneath the bottom right corner of panel L represents 50 microns and applies to all three images; RP: Red Pulp, WP: White Pulp, MZ: Marginal Zone, A: Artery.

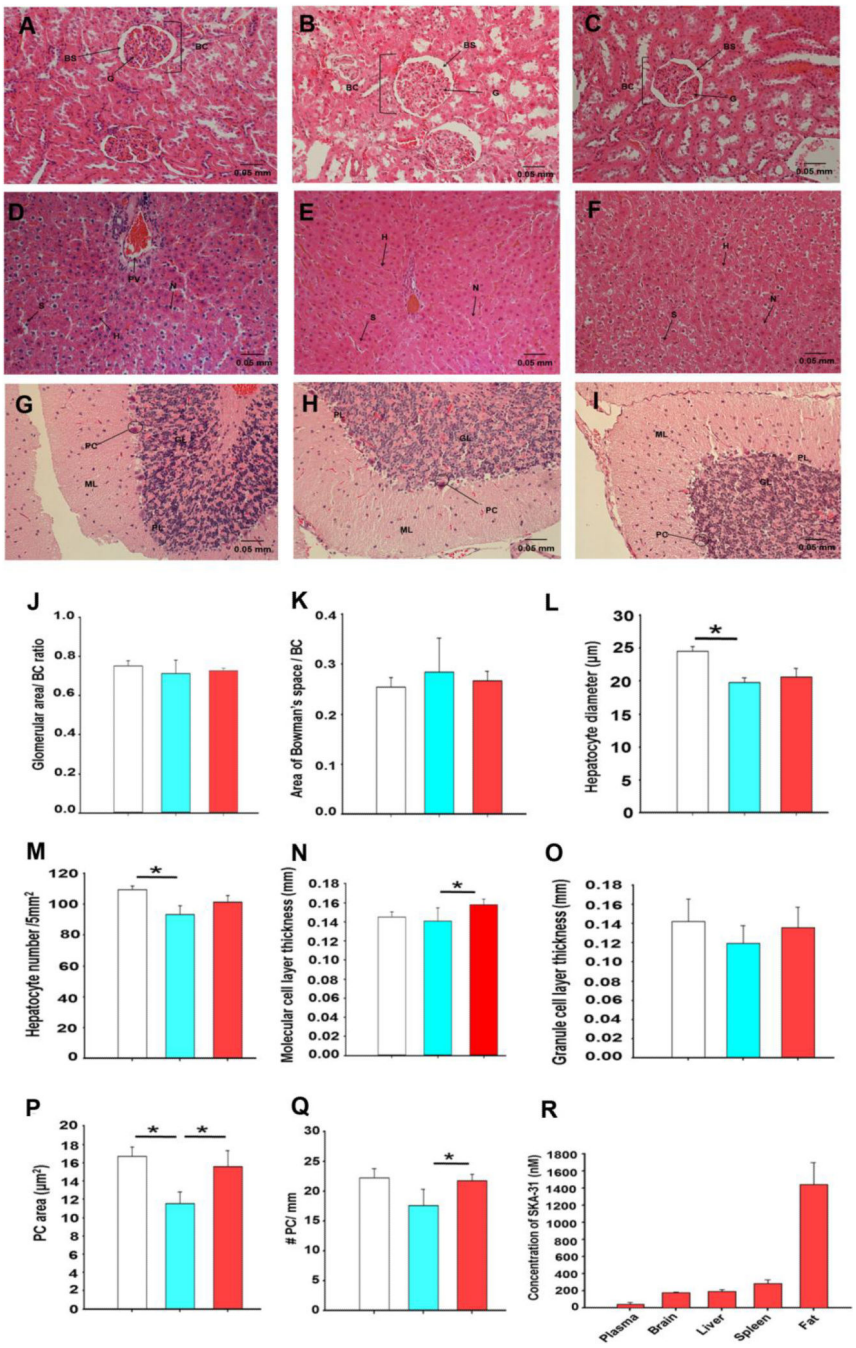

Figure 6 –. Long-term SKA-31 administration does not induce gross tissue damage.

Panels A-C display H&E histological staining of kidney sections (400x magnification) derived from vehicle treated young animals (A) and aged rats treated with either vehicle (B) or 10 mg/kg SKA-31 (C). BC: Bowman's capsule, BS: Bowman's Space, G: Glomerulus. H&E staining of liver sections (400x magnification) from vehicle treated young animals, and vehicle and SKA-31 treated aged rats is presented in panels D, E and F, respectively. H: Hepatocyte, N: Nucleus, S: Sinusoid, PV: Portal Vein. Panels G-I illustrate H&E staining of brain cerebellar sections (400x magnification) from vehicle treated young animals (G), and

vehicle (H) and SKA-31 treated aged rats (I). GL: Granule cell Layer, PC: Purkinje Cells, ML: Molecular cell Layer. The scale bar displayed in the bottom right corner of each image represents 50 microns. Quantification of select histological parameters in kidney, liver and cerebellum is presented in panels J-Q, as follows: glomerular size relative to area of Bowman's capsule (J), area of Bowman's space relative to Bowman's capsule (K), hepatocyte diameter (L), hepatocyte density per $5mm^2$ (M), molecular cell layer thickness in the cerebellum (N), granule cell layer thickness in the cerebellum (O), cerebellar Purkinje cell density per $5mm^2$ (P) and number of Purkinje cells per millimetre length of the molecular layer (Q). Structural measurements in stained sections were carried out using ImageJ software. White bars = vehicle-treated young rats, blue = vehicle treated aged rats, and red = SKA-31 treated aged rats. Statistical analyses were performed using one-way ANOVA and a Tukey's post-hoc test; the asterisk indicates a statistically significant difference between the indicated groups, $P < 0.05$ ($n = 6$ animals/group). The histogram in panel R shows the total plasma and tissue concentrations of SKA-31 in aged rats, as determined by LC/MS analysis. Tissues and plasma were collected at the time of euthanasia, approximately 18 hours following the final i.p. injection of SKA-31 ($n = 6$). Adipose (fat) tissue was obtained from the abdominal region. No SKA-31 was detected in material from vehicle treated animals.